PROCEEDINGS B

rspb.royalsocietypublishing.org

Research

Cite this article: Charvet CJ *et al*. 2017 Coevolution in the timing of GABAergic and pyramidal neuron maturation in primates. *Proc. R. Soc. B* **284**: 20171169.
http://dx.doi.org/10.1098/rspb.2017.1169

Received: 25 May 2017
Accepted: 21 July 2017

Subject Category:
Neuroscience and cognition

Subject Areas:
neuroscience

Keywords:
development, evolution, human

Author for correspondence:
Christine J. Charvet
e-mail: charvetcj@gmail.com

†Department of Molecular Biology and Genetics, Cornell University, 349 Biotechnology Building, Ithaca, NY, 14853.

Electronic supplementary material is available online at https://dx.doi.org/10.6084/m9.figshare.c.3843652.

THE ROYAL SOCIETY PUBLISHING

Coevolution in the timing of GABAergic and pyramidal neuron maturation in primates

Christine J. Charvet[1,2,†], Goran Šimić[3], Ivica Kostović[3], Vinka Knezović[3], Mario Vukšić[3], Mirjana Babić Leko[3], Emi Takahashi[1,4], Chet C. Sherwood[2], Marnin D. Wolfe[5] and Barbara L. Finlay[6]

[1]Division of Newborn Medicine, Department of Medicine, Boston Children's Hospital, Harvard Medical School, Boston, MA, USA
[2]Department of Anthropology and Center for the Advanced Study of Human Paleobiology, The George Washington University, Washington, DC, USA
[3]Department of Neuroscience, Croatian Institute for Brain Research, University of Zagreb School of Medicine, Zagreb, Croatia
[4]Athinoula A. Martinos Center for Biomedical Imaging, Massachusetts General Hospital, Harvard Medical School, Charlestown, MA, USA
[5]School of Integrative Plant Science, and [6]Evolutionary Neuroscience Group, Department of Psychology, Cornell University, Ithaca, NY, USA

CJC, 0000-0002-0985-3056

The cortex of primates is relatively expanded compared with many other mammals, yet little is known about what developmental processes account for the expansion of cortical subtype numbers in primates, including humans. We asked whether GABAergic and pyramidal neuron production occurs for longer than expected in primates than in mice in a sample of 86 developing primate and rodent brains. We use high-resolution structural, diffusion MR scans and histological material to compare the timing of the ganglionic eminences (GE) and cortical proliferative pool (CPP) maturation between humans, macaques, rats, and mice. We also compare the timing of post-neurogenetic maturation of GABAergic and pyramidal neurons in primates (i.e. humans, macaques) relative to rats and mice to identify whether delays in neurogenesis are concomitant with delayed post-neurogenetic maturation. We found that the growth of the GE and CPP are both selectively delayed compared with other events in primates. By contrast, the timing of post-neurogenetic GABAergic and pyramidal events (e.g. synaptogenesis) are predictable from the timing of other events in primates and in studied rodents. The extended duration of GABAergic and pyramidal neuron production is associated with the amplification of GABAerigc and pyramidal neuron numbers in the human and non-human primate cortex.

1. Introduction

Primates possess a relatively enlarged isocortex comprised of a greater density of isocortical neurons compared with many other studied mammals [1–6]. The relative expansion of isocortical neuron numbers in primates is accompanied by an absolute as well as a slight increase in the proportion of GABAergic interneuron numbers relative to studied rodents [7–10]. Evolutionary changes in isocortical neuron numbers and its cellular constituents have implications for cortical connectivity patterns and the computations it performs, the nature of which we do not yet fully understand [6,11,12].

Many distinctions can be made between cortical neuron classes, such as regions of axonal input and output, cell morphology, laminar position, and gene expression. Perhaps the most salient categorical distinction is between glutamatergic excitatory pyramidal neurons and inhibitory GABAergic interneurons. In this study, we identified developmental processes that could

produce coordinated expansion in the numbers of isocortical excitatory pyramidal and inhibitory GABAergic neurons in humans and macaques relative to rats and mice. These two cell classes differ in multiple ways. In addition to their defining difference in their computational role, pyramidal neurons preferentially project over long distances whereas GABAergic interneurons project locally [13–15]. Compared with the majority of other brain regions, however, pyramidal and GABAergic neurons are unusual as they reside in the same adult target region, the isocortex, but they are generated, largely, from distinct regions of the neural plate (electronic supplementary material, figure S1).

Pyramidal neurons arise from the developing cortical proliferative pool (CPP; electronic supplementary material, figure S1). These newly born neurons migrate to the cortical plate along radial glia according to the well-known 'inside out' sequence [16–19]. In mice as in primates, many GABAergic neurons originate from the ganglionic eminences (GE) and migrate to various layers of the developing cerebral cortex (electronic supplementary material, figure S1 [20–25]). GABAergic interneurons also migrate to a transitory zone situated between the intermediate and the cortical plate called the subplate, which partakes in the formation of intra- and extra-cortical connectivity [26]. In both primates and mice, some GABAergic interneurons are produced from the CPP in addition to the GE [22,27]. Given the difficulty in tracing embryonic migratory paths of these neurons, the relative numbers of isocortical neurons originating from the developing isocortical pool versus the GE have been difficult to ascertain in primates [26].

Previous comparative analyses of thymidine studies showed that isocortical neurogenesis extends for longer than expected in rhesus macaques relative to rats and mice [28,29]. An extended period of neurodevelopment could increase the vulnerability of primates to certain neurological disorders. In humans, imbalances in GABAergic and pyramidal neuron activity are a common theme of neurological disorders (e.g. anxiety disorders, epilepsy, intraventricular haemorrhage (IVH), schizophrenia [30–33]). Yet, we know very little about the basic developmental timeline of GABAergic and pyramidal neuron maturation in humans and other primates. One approach to understanding neurological disorders has been to use model organisms such as mice to recapitulate developmental dysfunctions that occur in humans. Although these studies are informative, they rely on assumptions of conservation between model organisms and humans [34]. Comparing key developmental parameters between primates and other mammals is an essential enterprise in order to relate findings from animal models to humans.

In this study, we demonstrate that the production of GABAergic interneurons and pyramidal neurons are selectively delayed in primates relative to other neurodevelopmental events. Species develop at different rates and so a comparative analysis of developmental timing of GABAergic and pyramidal events requires considering evolutionary changes in overall developmental schedules across species. We employed the translating time model to find the timing of equivalent developmental events across rhesus macaques, humans, and mice [28,29] and show that the timing of GE and CPP maturation is delayed in humans and macaques relative to the timing of other events. We also compared the timing of GABAergic and pyramidal events between humans, macaques, and mice after they exit the cell cycle to identify whether neurogenesis duration has an impact on the timing of subsequent maturation of GABAergic and pyramidal neurons. Although the GE and CPP grow for longer than expected in humans and macaques compared with mice, the timing of post-neurogenetic GABAergic and pyramidal events are not delayed in primates relative to rats and mice. Our findings demonstrate, for the first time, that selective delays in GE maturation and CPP maturation associate with the amplification of GABAergic interneuron and pyramidal neuron numbers in primates.

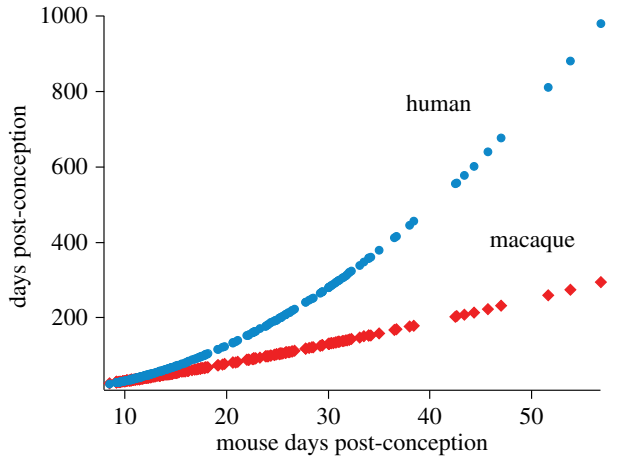

Figure 1. The timing of modelled events in humans and macaques are plotted against the timing of modelled events in mice. We use the timing of neural events to find equivalent maturational time points across humans, macaques, and mice [29]. Events that occur late in development occur progressively later in longer developing species such as humans. Isocortical neurogenesis timing, which is protracted in primates relative to studied rodents, is not included. (Online version in colour.)

2. Material and methods

The overall timing of developmental maturation varies among species. We used the translating timing model, which includes 271 neurodevelopmental events, with 1 010 data points from 19 mammalian species to find the timing of equivalent developmental events between rhesus macaques, humans, and mice (figure 1 [28,29]). We used these data to assess whether the growth of the CPP and GE are protracted in humans and macaques relative to mice (electronic supplementary material, figure S2 and figure 2).

During development, progenitor pools expand, peak, and wane. A number of studies have shown that the cell dense GE and CPP harbour mitotic cells [34,35]. A comparative analysis of growth trajectories can be used to identify whether the GE and CPP maturation are selectively delayed relative to other events in primates. We measured the GE and the cerebral CPP size of developing humans, macaques, and mice. The dataset consists of 17 mice (*Mus musculus*), 18 rhesus macaques (*Macaca mulatta*), 44 structural and eight high-resolution diffusion MR scans of prenatal humans (*Homo sapiens*). Some of these structural MRI scans are from atlases, which are averaged structural MRI across individuals (electronic supplementary material, table S1). Comparative analyses of growth trajectories of progenitor pools are instrumental in comparing neurogenesis timing between species [36].

We measured the GE and CPP size from Nissl-stained and HP-yellow-stained sections of mice and macaques made available by the Allen Institute for Brain Science. Brains of rhesus macaques and mice were cryoprotected in 4% sucrose, sectioned

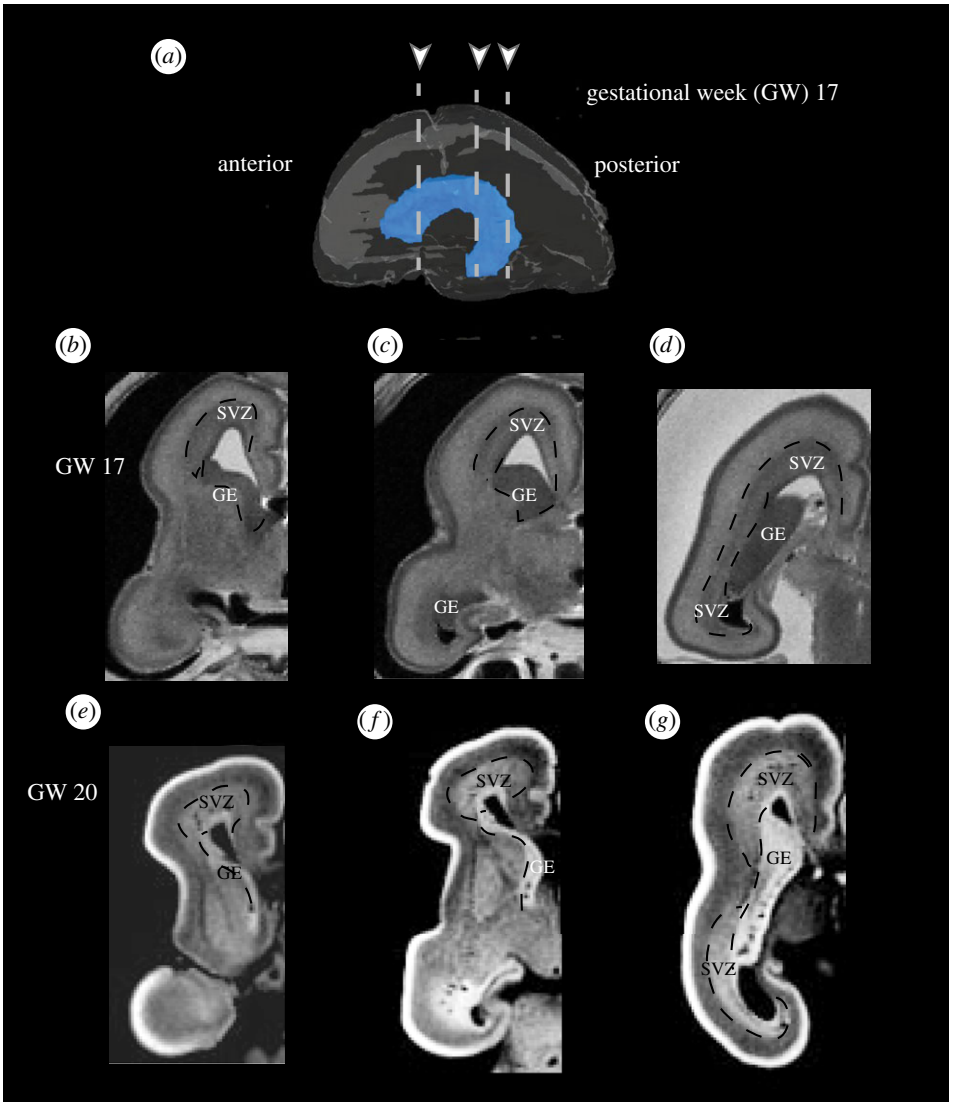

Figure 2. Three-dimensional reconstruction of the GE in a human fetus at gestational week (GW) 17. Arrowheads point to the approximate coronal planes shown for each fetus (*b*–*j*). Coronal slices of structural MRI scans of fetal humans at GW 17 (*b*–*d*) and GW 20 (*e*–*g*). The GE as well as the CPP (e.g. SVZ) are defined as a bright or dense region abutting the lateral ventricles. (Online version in colour.)

and stained. Selected macaques ranged between embryonic day (ED) 40 to birth. Mice used in the study ranged between post-conception day (i.e. ED) 12–20.5. These ages were chosen because they cover the period in which the GE is discernable and when it expands, peaks, and wanes.

We used high-resolution structural MRI scans to capture the growth of GE and CPP of humans. Few human embryonic brains are accessible for study and many of the human fetuses that are available for study have been paraffin-embedded and sectioned. This procedure causes brains to shrink. The extent of shrinkage may vary with age [36]. For these reasons, we measured the GE size from MRI scans rather than paraffin-embedded material. We obtained a large sample of 44 structural MRIs, which mostly include human fetuses ranging between GW 6 to birth. We also included two paediatric MRI scans. Structural MRI scans were obtained from several sources (electronic supplementary material, tables S1, S2, S3 [37–43]). MRI scans of six prenatal human brains with no anatomical malformations from the Zagreb collection [37] were imaged on a Siemens scanner. Ages and scanning protocols of these structural scans are listed in electronic supplementary material, tables S1 and S2. Four prenatal humans at GW 10, 12, 15, and 17 were imaged in a 4.7 T MRI system (Bruker Biospin GmbH, Germany). These high-resolution scans were used in a previous study and imaging protocols have been described previously [41]. If a progenitor pool was not clearly discernable from the structural MRI scan, it was not included in the analysis.

(a) Proliferative zone measurements

We measured the GE and CPP volumes at different stages of development in mice, macaques, and humans. The GE includes the medial, lateral, and caudal GE (electronic supplementary material, figures S1, S2 and figure 2). The GE and CPP are defined as a cell dense region from Nissl-stained sections, HP-yellow-stained sections, or structural MRI scans. Measurements of the CPP include those of the presumptive isocortex as well as the developing hippocampus, and include the ventricular zone, as well as the subventricular zones (electronic supplementary material, figure S2 and figure 2). To measure the volume of the GE and CPP, we selected 5–21 regularly spaced coronal, sagittal, or horizontal planes from MRI or histological material through the region of interest (ROI). Section spacing varied across individuals in accordance with specimen size. The GE and the CPP were outlined in each section, and area measurements were made with the software package ImageJ (Rasband 1997–2007). The sum of each region's cross-sectional area was multiplied by the distance between sections and section thickness to obtain the GE and CPP volume.

(b) High angular resolution diffusion magnetic resonance scans

Because the use of different MR scanning procedures may introduce noise in our analyses of growth trajectories in humans, we also used high-resolution diffusion MR scans of human fetuses as an alternative means to assess GE growth trajectories in humans. Eight brains ranging between the ages of GW 15–31 were imaged on a 4.7 T Bruker Biospec MR system (electronic supplementary material, table S3). Imaging protocols are described in detail in [42]. Brain samples were acquired from the Brigham and Women's Hospital and Children's Hospital Boston Departments of Pathology. Cases with known or suspected malformations were excluded from the study. We identified the GE from high angular resolution diffusion (HARDI) MR tractography as well as from fractional anisotropy scans [42–44]. We used a streamline algorithm for diffusion tractography as in previous publications [42,43]. The diffusion within the GE is strongly aligned along the anterior to posterior axis, which is in contrast with structures surrounding the GE [42]. We used these features to identify and quantify the growth of the GE from diffusion MRI scans. We placed a ROI through the GE with the software package TrackVis (http://trackvis.org) in order to visualize and quantify GE volume.

(c) Comparative analysis of GABAergic and pyramidal events

We asked whether delayed growth of the GE and CPP entails that subsequent post-neurogenetic GABAergic and pyramidal events occur later than expected in humans and macaques compared with mice. We collected developmental events in rats, mice, macaques as well as humans from the literature [29] to compare the developmental timing of GABAergic and pyramidal events in primates and in studied rodents (electronic supplementary material, table S4). Developmental events are rapid changes in developmental processes [28,29]. We collected data on the timing of GABAergic and pyramidal events. Interneurons express a distinct set of markers and have different embryological origins [13,14,20,24,25]. Accordingly, subpopulations of GABAergic interneurons may mature at different rates. To capture the maturation of this diverse class of neurons, we compared developmental changes in the timing of some of these molecular markers (e.g. calbindin, parvalbumin, calretinin) across species. Examples of GABAergic events include when parvalbumin expression is first observed in layers II–III. Examples of pyramidal events include myelination onset of the corpus callosum, and when cortical axons are first observed in the thalamus. We also obtained data on the timing of events, which may not be selective to GABAergic or pyramidal neurons but may be the result of maturational changes across both cell types (e.g. synaptogenesis). We excluded events related to isocortical neurogenesis because the timing of these events deviate from the timing of many other developmental events. Their inclusion could bias cross-species comparisons in developmental timing of GABAergic and pyramidal events. In total, we compared the timing of 250 developmental events between humans, macaques, rats, and mice. These developmental events consist of 28 GABAergic, 13 pyramidal, 20 general isocortical events, which could consist of GABAergic and pyramidal events. The dataset also consists of 189 other events across remaining brain regions.

In all cases, we obtained data for an event in at least one primate and at least one rodent. In a number of cases, we obtained the timing of an event for either a mouse or a rat but not for both rats and mice. That is, some developmental events do not have values for both rats and mice. A regression of the natural-logged values of developmental events of rats and mice shows strong covariation in the timing of events between these two species ($F = 1065$; adj $R^2 = 0.9325$; $p < 2.2 \times 10^{-16}$; $n = 79$), consistent with results from previous studies that show high predictability in the timing of events across species [28,29]. To increase power to detect developmental differences in GABAergic and pyramidal event timing between primates and studied rodents, we imputed developmental event timing in rats and mice for the missing data. We used a Monte Carlo simulation procedure implemented with the Mice package with the programming language R. We imputed developmental event timing across rats and mice with the predictive mean matching method with 80 iterations and 20 imputed datasets. We selected the imputed dataset, which showed the strongest correlation between the timing of events between rats and mice. We then combined imputed and observed developmental events from these two species. We regressed the timing of events in rats against the timing of events in mice. We extracted predicted values from this regression. We subtracted each value from the smallest value and divided each value by the difference between the greatest and smallest value. This produced an event scale with values, which ranged from 0 to 1. We regressed the natural-logged values of developmental event timing in humans on the event scale and the natural-logged values of developmental event timing in macaques versus the event scale. We then asked whether GABAergic and pyramidal events are protracted relative to other events in primates. We categorized events as either GABAergic, pyramidal-related located, or potentially both GABAergic and pyramidal events across the isocortex. We also included a fourth category, which includes events located in regions other than the isocortex. We performed an ANOVA on the residuals of events that were either GABAergic, pyramidal events, both, or from regions others than the isocortex.

3. Results

(a) Growth of the ganglionic eminences

The GE and CPP growth curves from a large sample of humans ($n = 44$), macaques ($n = 18$), and mice ($n = 17$) grow, peak, and subsequently wane with age (figures 3–5). At the earliest ages examined, the GE is roughly three to 13 times larger in humans and macaques than in mice. As development progresses, the GE grows and becomes more than 200 times larger in humans and macaques compared with mice (figure 3). These observations demonstrate that the GE and CPP expand by growing for longer than expected in humans and macaques compared with mice.

We compared the timing of GE and CPP peak size between humans, macaques, and mice because the peak volume represents a rapid transformation in developmental process, which can be readily compared across species. The GE peak size occurs between the ages of ED 15.5 to ED 16 in mice, ED 80 in the macaque, and between GW 21 and 27 in humans. The growth trajectories from high-resolution diffusion MR scans also demonstrate that the peak in GE size occurs between GW 20 and GW 21 in humans (figure 5). According to the translating time model, events occurring in mice on ED 16 are expected to occur on ED 59 in a macaque and on ED 81 in humans [29]. In humans as in macaques, the GE expands well beyond these equivalent developmental time points.

We assessed whether the growth of the GE is significantly protracted in humans and macaques relative to mice. To that end, we selected neural events that occur between ED 15 and

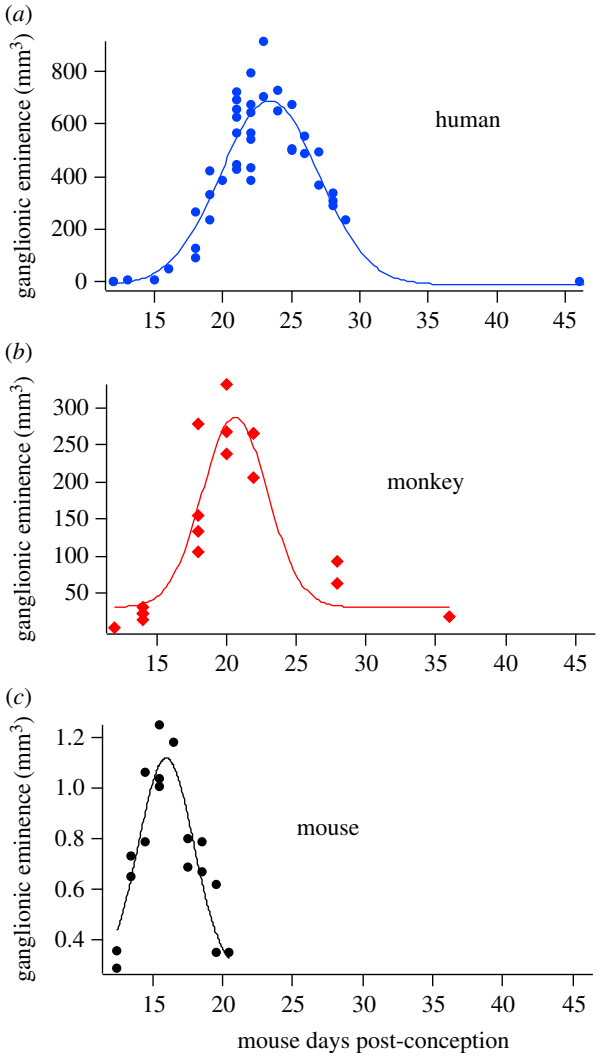

Figure 3. Growth of the GE in humans (*a*), macaques (*b*), and mice (*c*). Age in days after conception (embryonic days) of humans and macaques were translated to the age of mice [29]. A Gaussian function was fitted to the data. The peak size of the GE and CPP occur later than expected in humans and macaques compared with mice. (Online version in colour.)

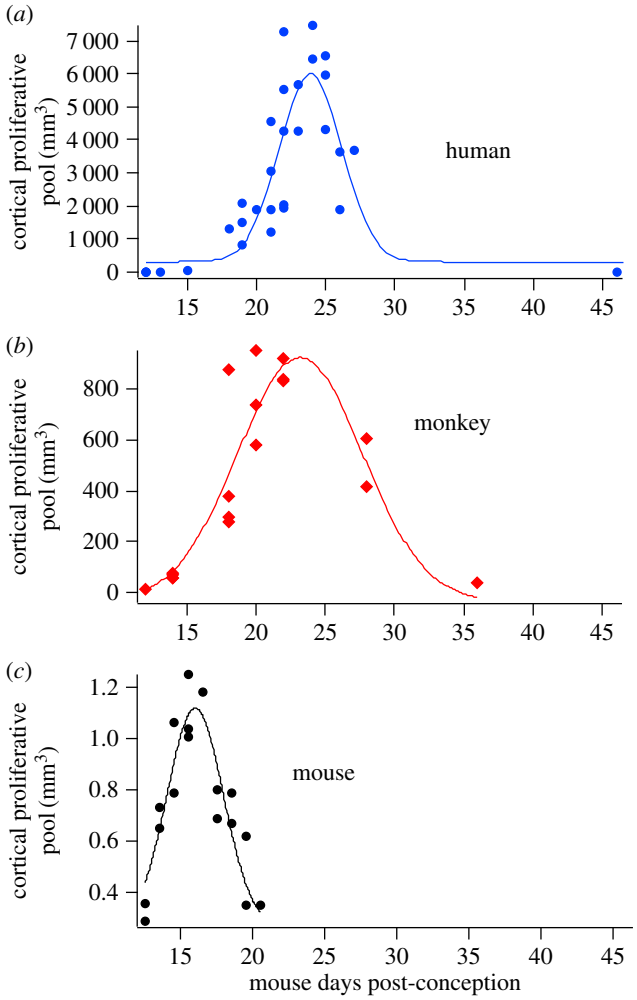

Figure 4. Growth of the CPP in humans (*a*), macaques (*b*), and mice (*c*). Age in days after conception (embryonic days) of humans and macaques were translated to the age of mice [29]. We fitted a Gaussian function to the data. The peak size of the GE and CPP occur later than expected in humans and macaques compared with mice. (Online version in colour.)

17 in mice from [29]. We identified when developmental events that occur between ED 15–17 in mice occur in humans and macaques to ask whether the timing of peak GE size in humans and macaques occur later than expected compared with mice. In these comparative analyses, we exclude events related to isocortical neurogenesis because isocortical neurogenesis is selectively protracted in macaques relative to rats and mice [29].

Events that occur between ED 15–17 in mice ($x = 15.85$; SE = 0.22; min = 15; max = 17; $n = 13$) occur on average on ED 61.9 in macaques (SE = 2.54; min = 45; max = 75; 95% CI: 46.5–72.25; $n = 12$). The peak size of the macaque GE occurs on ED 90, which is later than the upper 95% confidence interval (i.e. ED 72.25) of these data. Events that occur between ED 15–17 in mice occur on average on ED 104 in humans (SE = 25.02; min = 77; max = 154; 95% CI: 77.4–146.5; $n = 3$). The GE peak occurs between ED 161 to ED 168 in humans, which is later than the upper 95% confidence intervals (i.e. ED 146.5) of these data. Taken together, these findings demonstrate that the GE growth occurs for longer than expected in rhesus macaques and humans compared with mice. The protracted growth coupled with the expansion of the GE over developmental time are consistent with the notion that cells continue to cycle for longer in macaques and humans compared with mice.

(b) Growth of the cortical proliferative pool

We measured the volume of the CPP in rhesus macaques, humans, and mice to compare the timing of isocortical neurogenesis across these three species. The CPP grows for longer than expected in humans and rhesus macaques after controlling for overall differences in developmental schedules. The peak size of the CPP occurs between ED 14.5 and 15.5 in mice, on approximately ED 90 in macaques and on ED 182 in humans. Events that occur between ED 14.5–15.5 in mice occur on average on ED 58 in macaques (SE = 5.08; min = 48; max = 75; 95% CI= 48–72.6; $n = 5$). Events that occur between the ages of ED 14.5–15.5 in mice occur on average on ED 73.5 in humans (SE = 3.5; min = 70; max = 77; 95% CI = 70.35–76.65; $n = 2$). The CPP in humans and macaques continues to expand well beyond the 95% CI of these data. Each species also shows a strong correlation between CPP and GE volume over the developmental time periods examined (electronic supplementary material, figure S3; mice: $r^2 = 0.74$, $p < 0.01$; macaque: $r^2 = 0.92$, $p < 0.01$; humans: $r^2 = 0.84$; $p < 0.01$). Taken together, these findings

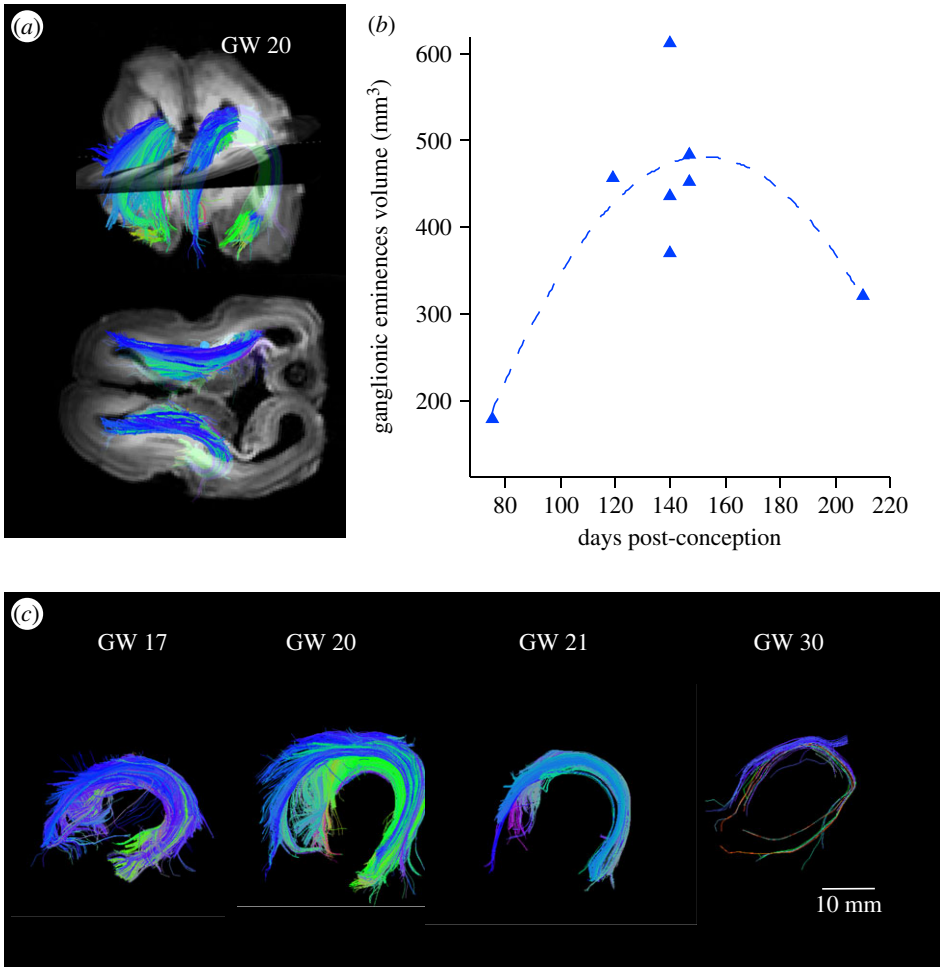

Figure 5. (*a*) Diffusion MR tractography of a human fetus at gestational week (GW) 20. The anisotropy of the GE is aligned along the anterior to posterior axis. (*b*) The GE expands at GW 21 and declines between the ages of GW 21–31. (*c*) MR tractography shows that the GE wanes between GW 21–31. Scale bar is 10 mm. (Online version in colour.)

demonstrate that the growth of the CPP and the GE covary within a species and continue to grow for significantly longer in macaques and humans relative to mice.

(c) Timing of GABAergic and pyramidal events

We next investigated whether the timing of GE and CPP growth predicts the timing of subsequent maturation of post-neurogenetic GABAergic and pyramidal events. We classified developmental events as either GABAergic events (e.g. changes in calbindin expression) or pyramidal (e.g. changes in neurofilament heavy polypeptide expression). Because some events could arise from maturational changes from both GABAergic and pyramidal events, we also classified a subset of these neural events into a third category, which could be the results of coordinated maturation of GABAergic and pyramidal neurons across the cerebral cortex (e.g. synaptogenesis, figure 6). We included the timing of events of brain regions other than the cerebral cortex and the GE as a fourth category. In total, we compared the timing of 157 developmental events between primates and studied rodents.

We regressed the natural-logged values of the timing of developmental events versus the event scale for each species. The event scale is a weighted average of ordered events, with early events with values close to 0 and late events with values close to 1. We found a very strong association between developmental events in humans and the event scale ($F = 372.5$, adj $R^2 = 0.836$; $p < 2.2 \times 10^{-16}$). We extracted residuals of events from the general linear model according to their category (i.e. GABAergic events, pyramidal events, coordinated maturation of isocortical GABAergic and pyramidal neurons, remaining brain regions). An analysis of variance of the residuals derived for each category in humans show that the timing of events are not significantly different from each other ($F = 0.103$, $p > 0.05$). We observed a similar situation when comparing macaques with rats and mice. That is, there is a strong association between the developmental event timing in macaques and the event scale ($F = 611.4$, adj $R^2 = 0.853$; $p < 0.01$). The residuals derived for each category are not statistically different from each other ($F = 1.927$; $p > 0.05$). Taken together, these findings demonstrate that an extension in progenitor pool maturation in primates does not entail protracted post-neurogenetic maturation of GABAergic and pyramidal events. Rather, the timing of post-neurogenetic pyramidal and GABAergic events conform to the timing of other events across the brain.

4. Discussion

The maturation of the GE and CPP in humans and macaques is relatively long compared with that in mice. The protracted growth of the GE and CPP associates with the coordinated expansion of GABAergic interneuron and pyramidal neuron numbers of the adult primate cortex [3,5–8]. Below, we outline evidence that supports this conclusion. We then

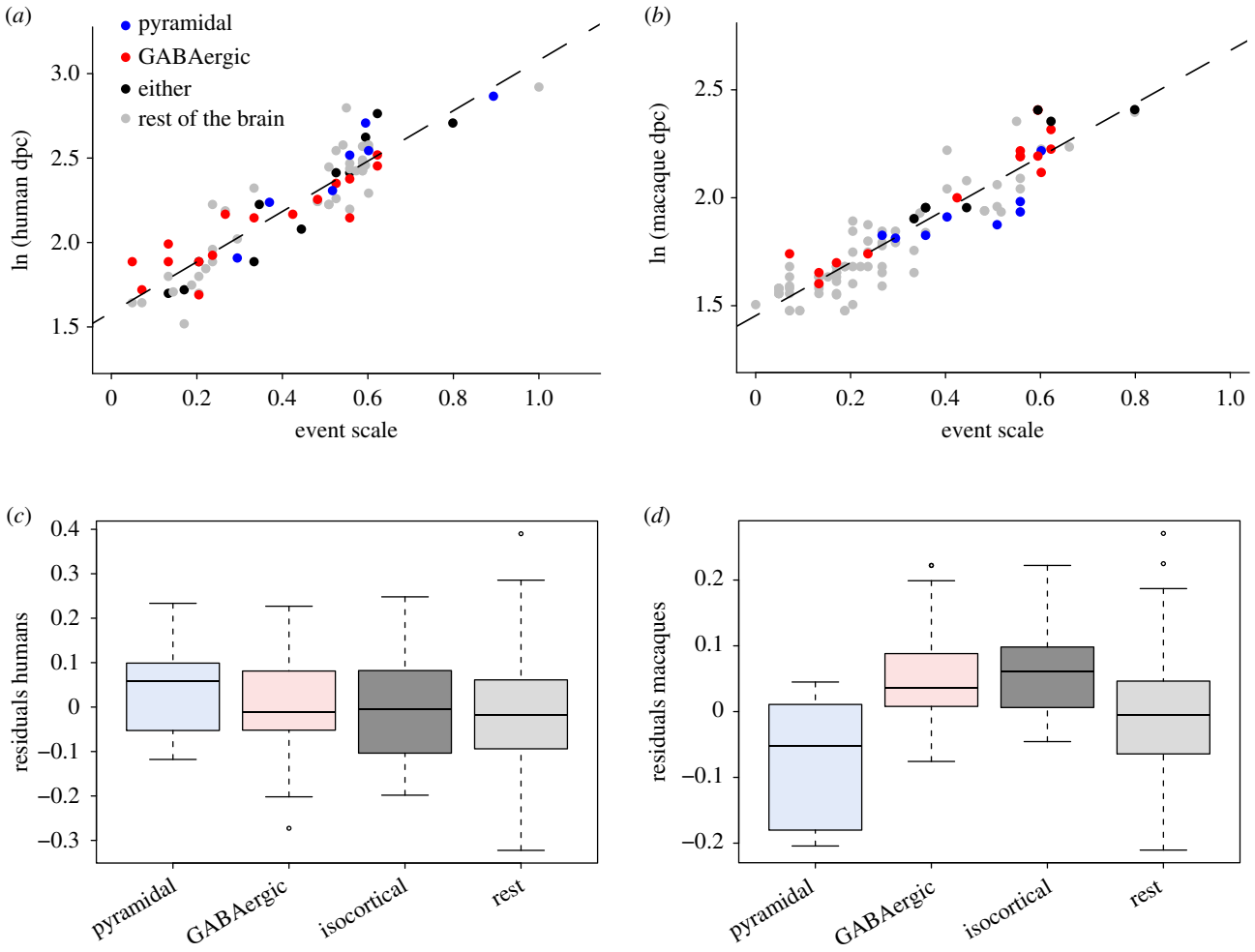

Figure 6. The timing of neural events expressed in days post-conception in humans (*a*) and macaques (*b*) are plotted against an event scale generated from the timing of events in rats and mice. Boxplots show the distribution of residuals derived from the linear regression for humans (*a*,*b*) and macaques (*c*,*d*). These data show that the timing of GABAergic and pyramidal events are similar to those of other events. These findings demonstrate that the timing of GABAergic and pyramidal post-neurogenetic events conform to the timing of other events in humans, macaques, rats, and mice. Dpc, days post-conception. (Online version in colour.)

discuss the implications of these results for the structure of the primate isocortex. We also highlight important developmental differences between primates and mice.

(a) Development of the ganglionic eminences and cortical proliferative pool

Previous comparative analyses of neurogenesis timing across species have used thymidine to birth-date neurons to show that isocortical neurogenesis occurs for longer than expected in macaques relative to a number of rodent species [17,28,29]. Cell birth-dating studies are lacking in humans and delays in neurogenesis have not been demonstrated previously in humans. Comparing CPP and GE growth curves in humans, macaques, and mice show that the CPP and GE grow for longer than expected in humans. The CPP and the GE wane around birth in mice and in humans, which coincides with when cortical neuron numbers reach adult levels [45–47]. These findings demonstrate, for the first time, that similar to macaques, humans selectively delay isocortical and GABAergic interneuron production relative to rats and mice.

There is a particular sequence in which neurons are generated in the isocortex. Neurons that exit the cell cycle early migrate to their final position in lower layers (i.e. layers V–VI) and neurons that exit the cell cycle late are located in upper layers (i.e. layers II–IV; [16]). Importantly, the production of neurons is not uniformly delayed in macaques relative to the timing of other events [29]. Neurogenesis onset is roughly equivalent between macaques and studied rodents at similar maturational stages but the duration of neurogenesis is extended in macaques compared with rats and mice. These findings are based on thymidine data, which is not a method that can be used to distinguish cells that are generated from the CPP from those that are generated from the GE [16–19]. Although neurogenesis onset and offset of lower layers occurs at equivalent maturational stages in the studied species, neurogenesis onset and offset of neurons of upper layer neurons occurs later than expected in macaques relative to studied rodents. In other words, cell cycle exit of all neurons located within upper layers, including GABAergic and pyramidal neurons, are delayed in macaques relative to rats and mice. These data are consistent with the results of the present study, which demonstrate that the proliferative pools giving rise to GABAergic and pyramidal neurons continue to grow for longer compared with the timing of other events. These lines of evidence converge to demonstrate that GABAergic and pyramidal neuron generation in primates are protracted relative to the timing of other events.

The GE and CPP peak in size between ED 80 to 90 in macaques. The peak size of these two proliferative pools coincides

with the major period of upper layer cortical neurogenesis in macaques. More specifically, in the primary visual cortex of the macaque, neurogenesis in layer IV begins at approximately ED 70, and ends on ED 85. Cell cycle exit of layers II–III neurons begins on ED 85 and ends on ED 100. Because the proliferative pool growth is protracted, and its size is maximal at around the ages in which upper layers are generated, upper layer neuron numbers should become disproportionately more numerous in primates relative to rats and mice. In line with these expectations, a previous study showed that layers II–IV neuron numbers are disproportionately more numerous in primates relative to studied rodents [6]. The expansion of upper layer neuron numbers in primates is the product of a prolonged production of neurogenesis.

(b) Protracted pool maturation has no obvious impact on the timing of subsequent events

We investigated whether delayed growth of progenitor pools entails that subsequent post-neurogenetic GABAergic and pyramidal events are delayed relative to other events in primates. The timing of GABAergic and pyramidal events conform to the timing of other developmental events across the brain in primates as well as rats and mice. The finding that delays in neurogenesis do not entail protracted maturation of subsequent developmental events is a first demonstrated example in which the timing of post-neurogenetic events are decoupled from the timing of neurogenetic events. This decoupling may facilitate coordinated cross-synaptic maturation across brain regions.

(c) Developmental origins of GABAergic interneurons

In infants born after less than 30 weeks of gestation, germinal haemorrhage is a common occurrence, occurring in 2.5/1 000 live births [48], often arises from the GE, can become manifest by 20 weeks of gestation, and is associated with suppressed cell proliferation [30]. Intraventricular haemorrhage (IVH) is associated with early deficits in attention, behavioural inhibition, and overall learning [49–52]. At the time that earlier studies described the occurrence of IVH, the fact that the GE were the source of telencephalic inhibitory neurons, or why this region seemed to be at risk in prematurity was not known. More recent studies suggest that the GABAergic population rather than pyramidal neurons are affected in IVH [34].

According to the timetable of neurogenesis and migration routes of GABAergic neurons characterized in mice, we would predict that a subset of GABAergic interneurons born around ages in which haemorrhages are observed are most affected in those individuals. Examining which GABAergic subtypes are most affected by these haemorrhages may serve to identify the developmental origins and timetable of GABAergic interneuron migration in humans. Rodent models of IVH should consider the developmental differences in the timing of GE maturation between humans and model organisms when translating findings from animal models to humans.

(d) Conclusion

The present study demonstrates that the growth of the CPP and GE are delayed relative to other events in primates. Imbalances in the electrophysiological properties of GABAergic and pyramidal neuron numbers are a common theme across a spectrum of neurological disorders (e.g. anxiety disorders, epilepsy, schizophrenia). Accordingly, our data suggests that the coevolution in the timing of GABAergic and pyramidal neuron maturation may be necessary for the circuitry to remain functional in evolution.

Data accessibility. All relevant data are in the electronic supplementary material.

Authors' contributions. C.J.C., B.L.F. designed the research; C.J.C. performed the research; GS, I.K., V.K., M.V., M.B.L., E.T. contributed data; C.J.C., M.D.W. analysed the data; C.J.C. wrote the paper; C.J.C., B.L.F., C.C.S., M.D.W. contributed to drafting the manuscript. All authors gave final approval for the publication.

Competing interests. The authors declare that we have no competing interests.

Funding. This work was supported by the James S. McDonnell Foundation (220020293) and the National Institutes of Health (R01 HD078561; R21 HD069001; R03 NS091587) to E.T. Some MRI scans of human fetuses housed at the Zagreb Neuroembryological Collection of Human Brains, which is funded by Unity Through Knowledge Fund (UKF) grant no. 1B06/07 and Croatian Science Foundation (CSF) grant. no. IP-2014-09-4517 to I.K. and CSF grant no. 7379 to M.V. G.Š. was funded by the CSF grant. no. IP-2014-09-9730.

Acknowledgements. Images of sectioned mice and macaques were taken from the Allen Institute Website and the Non-Human Primate (NHP) Atlas, respectively. These data are available at http://developing-mouse.brain-map.org and at http://www.blueprintnhpatlas.org/, which are supported by the NIH Contract HHSN-271-2008-00047-C to the Allen Institute for Brain Science. The opinions in this article are not necessarily those of the NIH. We thank Dr Brad Smith, University of Michigan (brdsmith@umich.edu) for extended access to prenatal human MRI scans available at http://embryo.soad.umich.edu/. Imaging was performed at the Center for In-Vivo Microscopy, Duke University and was funded by NIH N01-HD-6-3257 P/G F003637. We thank Fenna Krienen for helpful discussions.

References

1. Finlay BL, Hersman MN, Darlington RB. 1998 Patterns of vertebrate neurogenesis and the paths of vertebrate evolution. *Brain Behav. Evol.* **52**, 232–242. (doi:10.1159/000006566)
2. Barton RA, Harvey PH. 2000 Mosaic evolution of brain structure in mammals. *Nature* **405**, 1055–1058. (doi:10.1038/35016580)
3. Gabi M, Collins CE, Wong P, Torres LB, Kaas JH, Herculano-Houzel S. 2010 Cellular scaling rules for the brains of an extended number of primate species. *Brain Behav. Evol.* **76**, 32–44. (doi:10.1159/000319872)
4. Herculano-Houzel S. 2012 Neuronal scaling rules for primate brains: the primate advantage. *Prog. Brain Res.* **195**, 325–340. (doi:10.1016/B978-0-444-53860-4.00015-5)
5. Charvet CJ, Cahalane DJ, Finlay BL. 2015 Systematic, cross-cortex variation in neuron numbers in rodents and primates. *Cereb. Cortex* **25**, 147–160. (doi:10.1093/cercor/bht214)
6. Charvet CJ, Hof PR, Raghanti MA, van der Kouwe AJ, Sherwood CC, Takahashi E. 2017 Combining diffusion MR tractography with stereology highlights increased cross-cortical integration in primates. *J. Comp. Neurol.* **525**, 1075–1093. (doi:10.1002/cne.24115)
7. Beaulieu C. 1993 Numerical data on neocortical neurons in adult rat, with special reference to the GABA population. *Brain Res.* **609**, 284–292. (doi:10.1016/0006-8993(93)90884-P)

8. Beaulieu C, Kisvarday Z, Somogyi P, Cynader M, Cowey A. 1992 Quantitative distribution of GABA-immunopositive and -immunonegative neurons and synapses in the monkey striate cortex (area 17). *Cereb. Cortex* **2**, 295–309.
9. Sherwood CC *et al.* 2010 Inhibitory interneurons of the human prefrontal cortex display conserved evolution of the phenotype and related genes. *Proc. R. Soc. B* **277**, 1011–1020. (doi:10.1098/rspb.2009.1831)
10. Džaja D, Hladnik A, Bičanić I, Baković M, Petanjek Z. 2014 Neocortical calretinin neurons in primates: increase in proportion and microcircuitry structure. *Front. Neuroanat.* **8**, 103. (doi:10.3389/fnana.2014.00103)
11. Brodmann K. 1994. *Brodmann's 'Localization in the cerebral cortex'* (edited and transl. by LJ Garey). London, UK: Smith-Gordon.
12. Horvát S *et al.* 2016 Spatial embedding and wiring cost constrain the functional layout of the cortical network of rodents and primates. *PLoS Biol.* **147**, e1002512. (doi:10.1371/journal.pbio.1002512)
13. Rudy B, Fishell G, Lee S, Hjerling-Leffler J. 2011 Three groups of interneurons account for nearly 100% of neocortical GABAergic neurons. *Dev. Neurobiol.* **71**, 45–61. (doi:10.1002/dneu.20853)
14. DeFelipe J *et al.* 2013 New insights into the classification and nomenclature of cortical GABAergic interneurons. *Nat. Rev. Neurosci.* **14**, 202–216. (doi:10.1038/nrn3444)
15. Kepecs A, Fishell G. 2014 Interneuron cell types are fit to function. *Nature* **505**, 318–326. (doi:10.1038/nature12983)
16. Rakic P. 1974 Neurons in rhesus monkey visual cortex: systematic relation between time of origin and eventual disposition. *Science* **183**, 425–427. (doi:10.1126/science.183.4123.425)
17. Rakic P. 2002 Pre and post-development of neurogenesis in primates. *Clin. Neurosci. Res.* **2**, 29–32. (doi:10.1016/S1566-2772(02)00005-1)
18. Sanderson KJ, Weller WL. 1990 Gradients of neurogenesis in possum neocortex. *Brain Res. Dev.* **55**, 269–274. (doi:10.1016/0165-3806(90)90208-G)
19. Bayer SA, Altman J. 1991 *Neocortical development*. New York, NY: Raven Press.
20. Lavdas AA, Grigoriou M, Pachnis V, Parnavelas JG. 1999. The medial ganglionic eminence gives rise to a population of early neurons in the developing cerebral cortex. *J. Neurosci.* **19**, 7881–7888.
21. Nery S, Fishell G, Corbin JG. 2002 The caudal ganglionic eminence is a source of distinct cortical and subcortical cell populations. *Nat. Neurosci.* **5**, 1279–1287. (doi:10.1523/JNEUROSCI.0604-09.2009)
22. Letinic K, Zoncu R, Rakic P. 2002 Origin of GABAergic neurons in the human neocortex. *Nature* **417**, 645–649. (doi:10.1038/nature00779)
23. Ang ES, Haydar TF, Gluncic V, Rakic P. 2003 Four-dimensional migratory coordinates of GABAergic interneurons in the developing mouse cortex. *J. Neurosci.* **23**, 5805–5815.
24. Miyoshi G, Fishell G. 2011 GABAergic interneuron lineages selectively sort into specific cortical layers during early postnatal development. *Cereb. Cortex* **21**, 845–852. (doi:10.1093/cercor/bhq155)
25. Miyoshi G, Hjerling-Leffler J, Karayannis T, Sousa VH, Butt SJB, Battiste J, Johnson JE, Machold RP, Fishell G. 2010 Genetic fate mapping reveals that the caudal ganglionic eminence produces a large and diverse population of superficial cortical interneurons. *J. Neurosci.* **30**, 1582–1594. (doi:10.1523/JNEUROSCI.4515-09.2010)
26. Luhmann HJ, Kilb W, Hanganu-Opatz IL. 2009 Subplate cells: amplifiers of neuronal activity in the developing cerebral cortex. *Front Neuronat* **3**.
27. Petanjek Z, Berger B, Esclapez M. 2009 Origins of cortical GABAergic neurons in the cynomolgus monkey. *Cereb. Cortex* **19**, 249–262. (doi:10.1093/cercor/bhn078)
28. Clancy B, Darlington RB, Finlay BL. 2001 Translating developmental time across mammalian species. *Neuroscience* **105**, 7–17. (doi:10.1016/S0306-4522(01)00171-3)
29. Workman AD, Charvet CJ, Clancy B, Darlington RB, Finlay BL. 2013 Modeling transformations of neurodevelopmental sequences across mammalian species. *J. Neurosci.* **33**, 7368–7383. (doi:10.1523/JNEUROSCI.5746-12.2013)
30. Gonzalez-Burgos G, Lewis DA. 2008 GABA neurons and the mechanisms of network oscillations: implications for understanding cortical dysfunction in schizophrenia. *Schizophr. Bull.* **34**, 944–961. (doi:10.1093/schbul/sbn070)
31. Brambilla P, Perez J, Barale F, Schettini G, Soares JC. 2003 GABAergic dysfunction in mood disorders. *Mol. Psychiatry* **8**, 721–737. (doi:10.1038/sj.mp.4001362)
32. Hashimoto T, Arion D, Unger T, Maldonado-Avilés JG, Morris HM, Volk DW, Mirnics K, Lewis DA. 2008 Alterations in GABA-related transcriptome in the dorsolateral prefrontal cortex of subjects with schizophrenia. *Mol. Psychiatry* **13**, 147–161. (doi:10.1038/sj.mp.4002011)
33. Gallego Romero I *et al.* 2015 A panel of induced pluripotent stem cells from chimpanzees: a resource for comparative functional genomics. *Elife* **4**, e07103. (doi:10.7554/eLife.07103)
34. Del Bigio MR. 2011 Cell proliferation in human ganglionic eminence and suppression after prematurity-associated haemorrhage. *Brain* **134**, 1344–1361. (doi:10.1093/brain/awr052)
35. Arshad A, Vose LR, Vinukonda G, Hu F, Yoshikawa K, Csiszar A, Brumberg JC, Ballabh P. 2016 Extended production of cortical interneurons into the third trimester of human gestation. *Cereb. Cortex* **265**, 2242–2256. (doi:10.1093/cercor/bhv074)
36. Striedter GF, Charvet CJ. 2008 Developmental origins of species differences in telencephalon and tectum size: morphometric comparisons between a parakeet *Melopsittacus undulatus* and a quail *Colinus virgianus*. *J. Comp. Neurol.* **507**, 1663–1675. (doi:10.1002/cne.21640)
37. Judaš M, Šimić G, Petanjek Z, Jovanov-Milošević N, Pletikos M, Vasung L, Vukšić M, Kostović I. 2011 The Zagreb Collection of human brains: a unique, versatile, but underexploited resource for the neuroscience community. *Ann. NY Acad. Sci.* **1225**(Suppl 1), E105–E130. (doi:10.1111/j.1749-6632.2011.05993.x)
38. Gholipour A, Limperopoulos C, Clancy S, Clouchoux C, Akhondi-Asl A, Estroff JA, Warfield SK. 2014 Construction of a deformable spatiotemporal MRI atlas of the fetal brain: evaluation of similarity metrics and deformation models. *Med. Image Comput. Comput. Assist. Interv.* **17**, 292–299. (doi:10.1007/978-3-319-10470-6_37)
39. Zhan J *et al.* 2013 Spatial–temporal atlas of human fetal brain development during the early second trimester. *Neuroimage* **8**, 115–126. (doi:10.1016/j.neuroimage.2013.05.063)
40. Shi F, Yap P-T, Wu G, Jia H, Gilmore JH, Lin W, Shen D. 2011 Infant brain atlases from neonates to 1- and 2-year-olds. *PLoS ONE* **64**, e18746. (doi:10.1371/journal.pone.0018746)
41. Wang R, Dai G, Takahashi E. 2015 High resolution MRI reveals detailed layer structures in early human fetal stages: *in vitro* study with histologic correlation. *Front. Neuroanat.* **9**, 150. (doi:10.3389/fnana.2015.00150)
42. Miyazaki Y, Song JW, Takahashi E. 2016 Asymmetry of radial and symmetry of tangential neuronal migration pathways in developing human fetal brains. *Front. Neuroanat.* **10**, 2. (doi:10.3389/fnana.2016.00002)
43. Takahashi E, Folkerth RD, Galaburda AM, Grant PE. 2012 Emerging cerebral connectivity in the human fetal brain: an MR tractography study. *Cereb. Cortex* **22**, 455–464. (doi:10.1093/cercor/bhr126)
44. Vasung L, Jovanov-Milošević N, Pletikos M, Mori S, Judaš M, Kostović I. 2011 Prominent periventricular fiber system related to ganglionic eminence and striatum in the human fetal cerebrum. *Brain Struct. Funct.* **215**, 237–253. (doi:10.1007/s00429-010-0279-4)
45. Uylings, HBM, Malofeeva, LI, Bogolepova, IN, Jacobsen AM, Amunts, K, Zilles, K. 2005 No postnatal doubling of number of neurons in human Broca's areas (Brodmann areas 44 and 45)? A stereological study. *Neuroscience* **136**, 715–728. (doi:10.1016/j.neuroscience.2005.07.048)
46. Larsen CC, Larsen KB, Bogdanovic N, Laursen H, Graem N, Samuelsen GB, Pakkenberg B. 2006 Total number of cells in the human newborn telencephalic wall. *Neuroscience* **139**, 999–1003. (doi:10.1016/j.neuroscience.2006.01.005)
47. Fu Y, Rusznák Z, Herculano-Houzel S, Watson C, Paxinos, G. 2013 Cellular composition characterizing postnatal development and maturation of the mouse brain and spinal cord. *Brain Struct. Funct*. **218**, 1337–1354. (doi:10.1007/s00429-012-0462-x)
48. Robertson CM, Svenson LW, Joffres MR. 1998 Prevalence of cerebral palsy in Alberta. *Can. J. Neurol. Sci.* **25**, 117–122. (doi:10.1017/S0317167100033710)

49. Janowsky JS, Nass R. 1987 Early language development in infants with cortical and subcortical perinatal brain injury. *J. Dev. Behav. Pediatr.* **81**, 3–7. (doi:10.1097/00004703-198702000-00002)
50. Ross G, Tesman J, Auld PA, Nass R. 1992 Effects of subependymal and mild intraventricular lesions on visual attention and memory in premature infants. *Dev. Psychol.* **28**, 1067.
51. Christ SE, White DA, Brunstrom JE, Abrams RA. 2003 Inhibitory control following perinatal brain injury. *Neuropsychology* **17**, 171–178. (doi:10.1037/0894-4105.17.1.171)
52. Vasileiadis GT, Gelman N, Han VKM, Williams L-A, Mann R, Bureau Y, Thompson RT. 2004 Uncomplicated intraventricular hemorrhage is followed by reduced cortical volume at near-term age. *Pediatrics* **114**, e367–e372. (doi:10.1542/peds.2004-0500)